Energy 290 (2024) 130107

Contents lists available at ScienceDirect

Energy

journal homepage: www.elsevier.com/locate/energy

Modeling district heating pipelines using a hybrid dynamic thermal network approach

Saleh S. Meibodi [a], Simon Rees [b,*], Fleur Loveridge [b]

[a] Department of Engineering, Durham University, Durham, DH1 3LE, UK
[b] School of Civil Engineering, University of Leeds, Woodhouse Lane, Leeds, LS2 9JT, UK

ARTICLE INFO

Dataset link: https://doi.org/10.5518/1439

Keywords:
Dynamic thermal network
District heating
Buried pipes
Thermal response simulation

ABSTRACT

A novel numerical method is presented for fast and accurate simulation of the dynamic thermal behavior of buried pipelines such as those in district heating systems. The model is based on a combination of a conduction response factor method, known as the dynamic thermal network (DTN) method and a one-dimensional discretized heat transfer fluid flow model, the so-called plug flow N-continuously stirred tanks (PFST) model. This combination enables the model to effectively take into account the short timescale dynamic effects of pipelines including longitudinal dispersion of turbulent fluid and its thermal capacity and also transient ground heat transfer. The combined DTN-PFST model is validated by reference to experimental data from both the lab-scale representation of a district heating system and monitoring data from a full-scale operational system. The comparisons between simulation results and experimental data demonstrate a good level of accuracy of the proposed model in predicting the dynamic thermal behavior of pipelines. The model has also been found to be several orders of magnitude more computationally efficient than corresponding 3D numerical models. Both the accuracy and computational efficiency of the proposed model make it well-suited to the design and analysis of district heating distribution networks. The model is also expected to be well-suited to the modeling of horizontal ground heat exchange pipe systems.

1. Introduction

In recent decades district heating networks (DHN) have seen increased growth in both research effort and market deployment due to their proven benefits in terms of energy efficiency [1,2], greenhouse gas (GHG) emission reduction [3] and financial sustainability [4]. The ability to integrate various renewable energy sources, such as solar [5] and geothermal energy [6] along with low exergy heat sources [7] and industrial excess heat [8] make such technology key to the decarbonization of heating in the building sector. Recently, new concepts of ultra-low temperature district heating systems [9] and fifth generation district heating and cooling (5GDHC) systems [10–12] have been proposed aiming to improve district heating performance and promote further uptake of such technology.

One of the common characteristics of the concepts of modern heat networks is reduced operating temperature levels to not only decrease the network heat losses, but be able to integrate more low-temperature heat sources. This raises new technical challenges for the district heating networks to effectively deal with the large share of the intermittent and fluctuating low-temperature energy inputs while fulfilling the dynamic thermal energy requirements of energy users connected to the network. Consequently, proper dynamic network modeling is crucial in both the early design stage and optimization to ensure sufficient thermal energy can be delivered to the energy consumers through the pipeline systems at the same time minimizing carbon emissions [13,14].

There is significant existing research dealing with modeling distribution networks with a focus on heat transport through pipelines [15–18]. In general, the simulation of heat propagation through the district heating pipelines is carried out using two main approaches: black box methods and physics-based deterministic methods. In the former, the inputs and outputs of the pipe system which are deemed as a package are considered in the calculation. Stochastic models such as Artificial Neural Networks (ANN), are applied in black box approaches to deal with the non-linear characteristics of fluid flow and heat transfer of the pipe systems [19,20]. On the other hand, in physics-based deterministic methods, combinations of hydraulic and thermal models are employed to directly describe the flow and heat transfer of the pipe systems given detailed design parameters. Deterministic physics-based models of buried pipe systems are comprehensively reviewed by Talebi et al. [21] and Sarbu et al. [22].

* Corresponding author.
E-mail address: s.j.rees@leeds.ac.uk (S. Rees).

https://doi.org/10.1016/j.energy.2023.130107
Received 19 June 2023; Received in revised form 17 November 2023; Accepted 21 December 2023
Available online 22 December 2023

Nomenclature

A	Surface area, m^2
C	Specific heat capacity, kJ kg^{-1} K^{-1}
D	Diameter, m
f	Friction factor
h	Heat transfer coefficient, W m^{-2} K
K	Conductance, W K^{-1}
$\bar{K}$	Modified conductance, W K^{-1}
L	Length, m
$\dot{m}$	Mass flow rate, kg s^{-1}
n	Surface normal
N	Number of surfaces or tanks
Pe	Peclet Number
Pr	Prandtl Number
Q	Heat transfer rate, W
$\bar{Q}$	Average heat transfer rate, W
r	Pipe radius, m
R	Thermal resistance, K W^{-1}
Re	Reynolds Number
t	Time, s
Δt	Time step size, s
T	Temperature, °C
$\bar{T}$	Weighted average temperature, °C
v	Velocity, m s^{-1}
x	Position (coordinate), m

Greek symbols

ϵ	Effectiveness
κ	Weighting function or factor
λ	Thermal conductivity, W m^{-1} K^{-1}
ρ	Density, kg m^{-3}
τ	Time (integration variable), s

Subscripts

a	Admittive
e	Environment
f	Fluid
i, j	Surface number
in	Inlet
m, n, q	Index
out	Outlet
p	Pipe
t	Transmittive

Acronyms

4GDH	4th Generation District Heating
5GDH	5th Generation District Heating
ADPF	Axial Dispersion Plug Flow
DH	District Heating
DTN	Dynamic Thermal Network
DTN-PFST	Dynamic Thermal Network - Plug Flow Stirred Tank
FVM	Finite Volume Method
NTU	Number of transfer units
PF	Plug Flow
PFST	Plug Flow Stirred Tank

In black box approaches, the calculations are carried out based on stochastic mathematical functions between inputs and outputs, and parameters are developed using testing against a database consisting of experimental data or obtained from other types of numerical solutions. The main advantage of this approach is the low computational cost of modeling the systems. However, in conditions where a database does not provide sufficient data, the model fails to accurately predict the behavior of the pipe systems. Consequently, the applicability of the model is limited to cases with a large amount of available training data [23].

Deterministic models have the advantage of being readily adapted based on engineering design and environmental parameters. Such models are available with different levels of spatial and temporal resolution. The common physical approaches used for detailed two or three-dimensional pipeline modeling are the Finite Element Method (FEM) [24] or the Finite Volume Method (FVM) [25,26]. However, The main restraint of employing coupled 2D or 3D thermo-fluid dynamic models is the relatively high computational time required to solve the governing equations in both solid and fluid domains. To overcome this issue, several approaches have been proposed to effectively represent physical processes with reasonable computational cost with acceptable accuracy [16,23,27].

One type of approach is to discretize the pipe in one dimension and consider the inlet and outlet temperature of the pipe (nodes) and propagation delay depending on the fluid velocity, and solve the heat balance equation for the nodes taking into account the variation of pipe wall temperature and its thermal resistance [28]. This is the so-called node method and is used mainly for long pipes where the number of nodes used is determined depending on the spatial scale and Courant number [29]. It should be noted that this method is different from the so-called element method [30] in which the pipe is spatially discretized, but often introduces numerical artificial diffusion. Palsson [31] implemented these two methods to model the dynamic temperature response of DH pipes and analyzed the numerical results. He concluded that the node method is superior to the element method from both accuracy and computational cost points of view.

The node approach can also be adopted in a number of computational tools. Giraud et al. [32] presented a Modelica library [33] for modeling DH pipes using the node method called 'NodeMethodPipe' and validated the model experimentally using long time series data. In another study, Sartor and Dewalef [15] proposed a node model that took into account the thermal inertia of the pipes and the heat losses and implemented this in the TRNSYS software library [34]. There are a number of similar approaches focused on modeling the dynamic response of district heating pipe fluid [16,17,35] but which neglect transient conduction heat transfer with the surrounding ground and the effects of atmospheric conditions.

Furthermore, simulation of dynamic thermal responses of pipelines (ignoring ground heat transfer) can be carried out using methods developed for chemical engineering applications using one-dimensional fluid flow advection–dispersion modeling: the so-called Axial Dispersion Plug Flow (ADPF) [36]. It has been shown that by applying the ADPF model, the dispersion of turbulent fluid flow of the chemical concentration species [37] as well as heat [38] in pipelines can be successfully modeled. In such models, the physical diffusion processes relating to the multidimensional variations in the fluid velocity and temperature distribution are approximated by one-dimensional discretization. To that end, the pipeline is divided into a series of finite well-mixed elements, i.e. stirred tanks, and the time-varying temperatures of each stirred tank are derived by applying the energy balance to each tank in turn in the direction of fluid flow. This method has been applied and validated to model the dynamic thermal response of conduits [39] and borehole heat exchangers [40,41].

Recently, Meibodi and Rees [42] developed and validated a new ADPF model to predict short-time-scale dynamic thermal responses of pipelines with and without insulation. This model is a combination of a plug flow model (PF) to accurately represent the time delay and a number of continuously stirred tanks (ST) in series to represent the axial diffusion process in pipelines. It was demonstrated that this so-called

Plug Flow Stirred Tanks (PFST) model is well-suited to simulation of heat propagation through pipelines in that it short timescale dynamic effect results are well matched with experimental data. This approach overcomes the problems of excessive longitudinal diffusion known to be inherent in ADPF models [43].

Although the one-dimensional advection–dispersion modeling approach was successfully verified and validated by experimental data for such cases, it is only applicable for the simulation of short-timescale thermal responses of pipes where radial heat losses are calculated using steady-state thermal resistances between fluid, the pipes, and the environment. Some extension is required to deal with ground heat transfer. Abugabbara et al. [44] implemented a district heating pipeline model using a multipole analytical model to represent steady-state heat transfer as a delta configuration of three thermal resistances between the supply and return pipes and the ground along with a node in a discretized pipe element. This amounts to a steady-state heat transfer model and ADPF discretization of the pipe, and so has some of the limitations of both types of submodels. Hirsch and Nicolai [45] also arrived at a discretization equivalent to the ADPF approach, but sought to address shortcomings in modeling 5GDH systems with regard to static flows and fluid conditions at low temperatures.

For district heating pipelines that are typically buried at a depth of approximately 2 m, neglecting surrounding ground temperature variations driven by a combination of environmental conditions and prior seasonal heat loss, is not realistic. Consequently, one of the objectives of this study has been to develop a model with the ability to include time-varying atmospheric conditions on the exposed ground surface and deal with the long-term dynamics of seasonal ground heat exchange in an accurate and computationally efficient way. Although adapting pipeline fluid flow and heat transfer models to include steady-state representation of the ground, albeit with time-varying boundary conditions, gives some representation of ground heat losses, this does not account for the transient nature of ground heat transfer. For example, such adaptations ignore the time lag between atmospheric conditions and ground temperatures at the depths at which pipes are typically installed, which are of the order of several weeks due to the thermal capacity of the ground: a fully transient modeling approach is required to capture such effects.

With these aims, the PFST model of fluid flow has been combined with the Dynamic Thermal Network (DTN) method to represent the complex transient conduction processes between the time-varying temperatures of buried district heating pipelines and ground surfaces. The DTN approach is a response factor method in which dynamic conduction processes can be represented in terms of boundary temperatures and heat fluxes as a network of nodes denoting the surfaces linked via thermal resistances. The approach was first developed by Claesson et al. [46] as an extension of network representations of steady-state conduction processes for the transient simulation of heat transfer in building structures and components.

In the DTN approach, any complex three-dimensional geometry with heterogeneous properties can be dealt with: something difficult in analytical conduction heat transfer models. The method has been shown [46] to be mathematically exact with piece-wise varying boundary conditions in its discrete form. These particular advantages have motivated the implementation of the method in modeling the long-term thermal performance of numerous thermal engineering applications such as energy piles [47], foundation heat exchangers [48] and diaphragm wall ground heat exchangers [49].

The Dynamic Thermal Network (DTN) method falls into the category of response factor approaches in that it seeks to represent dynamic conduction heat transfer in terms of current and past temperatures according to pre-determined weighting factors. Many such response factor approaches are inherently one-dimensional. The main advantages of the DTN approach are the ability to represent any arbitrary three-dimensional geometries with heterogeneous thermal properties and the computational efficiency and robustness in dealing with the time-varying boundary conditions at multiple surfaces in bodies of significant thermal capacity. The method is well suited to modeling building components and ground heat exchange systems where there is an interest in simulating over long time scales. Full details of the DTN method and formulation are given elsewhere [50] and a brief overview is provided below.

A particular feature of the DTN approach is that, given pre-calculated weighting factors, the final equations are simple and so can be efficiently solved. The weighting response factors can be derived from the analysis of the heat fluxes in response to a step change in boundary temperatures. Although the derivation of required response factors may take some effort, particularly for a complex three-dimensional problem, once the values are calculated they can be stored for later use in simulations. It should be noted the DTN method does not rely on the way that the required weighting response factors are derived and hence the most convenient way of the derivation of response factors can be selected depending on the complexity of the geometry and variation in thermal properties. Such methods include a wide range of numerical models [48] and analytical models [51] as well as experimental data [18]. In this research, a finite volume method (FVM) has been used to generate the step response heat flux history required for the derivation of weighting factors and will be discussed in detail in Section 2.4

In this study, a model denoted as the combined dynamic thermal network and plug flow with stirred tanks (DTN-PFST) model is developed and we introduce the formulation below. The intention in combining these modeling approaches is that the advantages in modeling ground heat transfer of the DTN model are added to the advantages in modeling longitudinal transport effects of the PFST model. This is to represent the physical phenomena occurring in buried pipe systems more fully and accurately than existing approaches.

2. Model development

An overview of the representation of the dynamic thermal network (DTN) model of district heating pipeline systems is given in the following Section 2.1. An explanation is given of application of time-varying boundary conditions of pipelines to the DTN model is presented in Section 2.2. Subsequently, the details of the one-dimensional discretized model, the so-called plug flow with stirred tanks (PFST) model, is presented along with the new combined DTN-PFST model. Its application to district heating pipeline systems is presented in Section 2.5. The combined DTN-PFST model has been verified and validated against experimental data from both lab-scale (refer to Section 3) and full-scale district heating facilities as we elaborate in Section 4.

2.1. Dynamic Thermal Network representation

The concept of representing heat transfer as a network of nodal temperatures and resistances is extended in the DTN approach to deal with transient conditions where the heat fluxes are driven by time varying boundary temperatures [46,51–53]. In the context of district heating pipes we treat heat transfer in the ground as taking place only by conduction according to Fourier's Law. This can be formulated with constant properties and a set of N boundary conditions of the mixed type with constant surface heat transfer coefficients, h,

$$\nabla \cdot (\lambda \nabla T) = \rho C \cdot \frac{\partial T}{\partial t} \tag{1}$$

$$h_i \cdot \left[T_i(t) - T|_{A_i} \right] = \lambda \cdot \frac{\partial T}{\partial n}, \quad [i = 1 \dots N]$$

In problems of this type, the primary interest is in the relationship between boundary fluxes and temperatures rather than ground temperatures per se. Given a solution for the boundary temperatures, the boundary heat fluxes of interest associated with surface i of area S_i, can be calculated using,

$$Q_i(t) = A_i \cdot h_i \cdot \left[T_i(t) - T|_{A_i} \right] \tag{2}$$

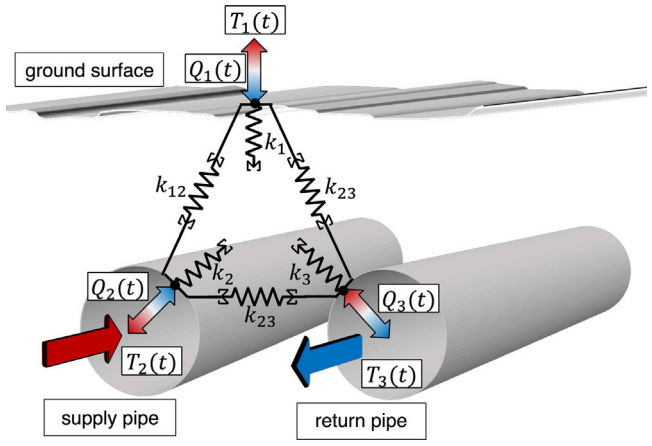

Fig. 1. Dynamic thermal network representing the buried flow and return pipes and the ground boundary for a unit installed length.

District heating pipeline systems can be represented as a three-surface application in the DTN method where time-varying boundary conditions are applied at three surfaces: supply and return pipelines and ground surfaces. The network consequently has a delta form with three nodes and three heat transfer pathways. Fig. 1 displays the DTN representation of district heating pipelines where the supply pipe and return pipe boundaries are nodes with time-dependent temperatures $T_2(t)$ and $T_3(t)$ respectively and heat flows at the pipe/ground boundary (coupling at the interface with the pipe model will be discussed in a later section) and at the ground upper boundary which is represented by a third node with time-dependent temperature $T_1(t)$. The temperatures, $T_i(t)$, and heat fluxes, $Q_i(t)$, of the dynamic network are specified at boundary temperature nodes with convective (mixed) boundary conditions rather than at the surfaces themselves. (The terms "boundary" and "surface" are distinguished in subsequent discussion). The reversed summation symbols (Σ) adjacent to the conductances in Fig. 1 are shown to indicate the average (weighted) current and previous temperatures at the boundaries are used in the DTN calculation. The conductances are constant values directly related to those in the corresponding steady-state network representation.

A fundamental feature of the DTN approach is that heat fluxes at each boundary are defined by a combination of time-varying admittive and transmittive components. Admittive fluxes are associated with the temperature variations at that boundary, while transmittive fluxes are associated with the temperature differences between two adjacent boundaries. Two types of conductance are defined in the DTN approach: the surface thermal conductances associated with the admittive path indicated with a single subscript (K_i) and other thermal conductances associated with the transmittive path between a pair of surfaces indicated with double subscripts, K_{ij}.

The surface conductances are constant values that can be calculated by multiplying the surface area (A_i) and the heat transfer coefficient (h_i) i.e., $K_i = A_i h_i$. The transmittive conductances are equivalent to the inverse of the steady-state thermal resistance between the two surfaces, i.e., $K_{ij} = 1/R_{ij}$. These may be calculated analytically is some simple cases but for more complex geometries, such as this application, numerical methods are more appropriate.

For the case of district heating pipelines, there are three surface thermal conductances (K_1 and K_2, K_3) for the ground, supply and return pipes surfaces, respectively, and three thermal conductances between the pipe and ground surfaces (K_{12} and K_{13}, K_{23}), as illustrated in Fig. 1. These constants are directly related to the surface and total conductances in the related steady-state network. It is the definitions of the average temperatures in the network that account for representation of transient behavior and properties.

For the three-node heat transfer network used to represent the district heating pipeline application, the heat flux at each surface consists of one admittive heat flux (Q_{1a} etc.) and two transmittive heat fluxes (Q_{12}, Q_{13} etc.), so that the heat balance equations can be expressed as follows:

$$\begin{aligned} Q_1(t) &= Q_{1a}(t) + Q_{12}(t) + Q_{13}(t) \\ Q_2(t) &= Q_{2a}(t) + Q_{21}(t) + Q_{23}(t) \\ Q_3(t) &= Q_{3a}(t) + Q_{31}(t) + Q_{32}(t) \end{aligned} \tag{3}$$

Although the general DTN formulation does not rely on any particular form of excitation it is helpful to appreciate the relationship between the admittive and transmittive fluxes by considering application of a step change in temperature at one of the boundaries. Consider the response for pair of buried district heating pipes with three boundaries defined as in Fig. 1 when all material and surfaces start with zero temperature and a step change in boundary temperature is applied at the return pipe surface (3) and the temperature at the ground and flow pipe boundaries (1 and 2) are held at zero. At the beginning of the step change, the flux at the pipe boundary being excited (Q_3) is entirely admittive in nature ($Q_3 = Q_{3a}$ at $t = 0$) and is limited by the surface conductance K_3 ($= h_3 A_3$). As steady-state is approached, the admittive component approaches zero and the transmittive flux to the other two boundaries approaches their steady-state value. At any time, the admittive component is given by the difference between the total flux and the sum of the transmittive fluxes with the other boundaries. The nature of time-varying fluxes in this situation are indicated in Fig. 2. The steady-state pipe flux can be seen to be balanced by the combination of flow pipe and ground fluxes at any time.

Claesson [52] showed that the temperature differences driving the absorptive and transmittive fluxes can be always defined in an exact manner by the current and weighted averages of the boundary temperatures. The absorptive and transmittive fluxes at a given boundary can be written in terms of the conductances and these temperatures as follows,

$$Q_{ia}(t) = K_i \cdot \left(T_i(t) - \int_0^\infty \kappa_{ia}(\tau) \cdot T_i(t-\tau)\, d\tau \right) \tag{4}$$

$$Q_{ij}(t) = K_{ij} \cdot \int_0^\infty \kappa_{ij}(\tau) \cdot \left[T_i(t-\tau) - T_j(t-\tau) \right] d\tau \tag{5}$$

where τ is a integration variable for time. The temperatures are averaged according to weighting functions, κ_{ia} and κ_{ij} for the admittive flux at the surface and the transmittive flux between surfaces respectively. A shorthand notation is used to denote these weighted average temperatures as follows,

$$\bar{T}_{ia}(t) = \int_0^\infty \kappa_{ia}(\tau) \cdot T_i(t-\tau)\, d\tau \tag{6}$$

$$\bar{T}_{ij}(t) = \int_0^\infty \kappa_{ij}(\tau) \cdot T_i(t-\tau) d\tau \tag{7}$$

The absorptive and transmittive fluxes in Eq. (3) can then be expressed in terms of these current and weighted averages of the boundary temperatures as well as the thermal conductances, as follows [46]:

$$\begin{aligned} Q_1(t) &= K_1[T_1(t) - \bar{T}_{1a}(t)] + K_{12}[\bar{T}_{12}(t) - \bar{T}_{21}(t)] \\ &\quad + K_{13}[\bar{T}_{13}(t) - \bar{T}_{31}(t)] \\ Q_2(t) &= K_2[T_2(t) - \bar{T}_{2a}(t)] + K_{12}[\bar{T}_{21}(t) - \bar{T}_{12}(t)] \\ &\quad + K_{23}[\bar{T}_{23}(t) - \bar{T}_{32}(t)] \\ Q_3(t) &= K_3[T_3(t) - \bar{T}_{3a}(t)] + K_{12}[\bar{T}_{21}(t) - \bar{T}_{12}(t)] \\ &\quad + K_{23}[\bar{T}_{32}(t) - \bar{T}_{23}(t)] \end{aligned} \tag{8}$$

where $\bar{T}_{ia}(t)$ are the admittive weighted average temperatures, and $\bar{T}_{ij}(t)$ are the transmittive weighted average temperatures. It can be shown that in the steady-state condition, each average temperature is equal to the related boundary temperature ($\bar{T}_{ia} = \bar{T}_{ij} = T_i$). Hence, Eq. (8) reverts to the general relationships between the overall conductances and boundary temperatures in the steady-state conditions, e.g. $Q_1 = K_{12}[T_1 - T_2] + K_{13}[T_1 - T_3]$.

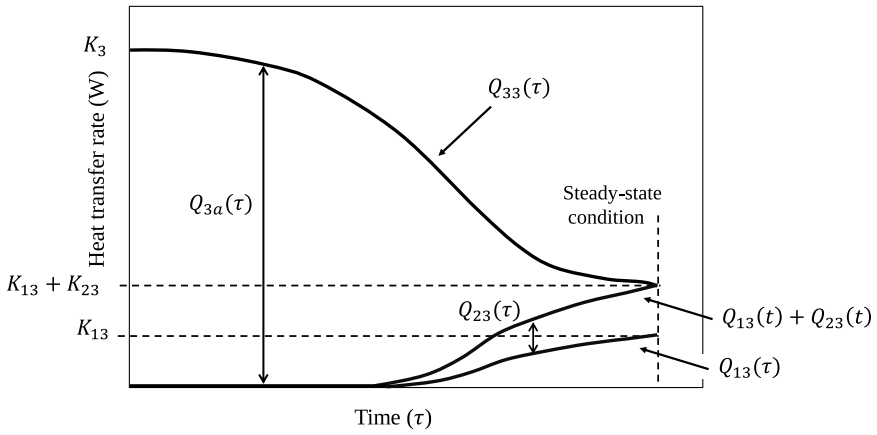

Fig. 2. Character of the step response boundary fluxes for a typical heat network return pipe.

2.1.1. DTN model discretization and step response data

In general [46], there are exact weighting functions related to the differentials of the time-varying fluxes (differentiating Eqs. (4) and (5)). In simulation applications, it is more convenient to use a discretized form of the DTN equations and use weighting factors rather than weighting functions and node temperatures at fixed time steps. The equations remain exact when the boundary conditions change in a piece-wise linear manner. A convenient way to derive weighting factors is to apply step changes to boundary temperatures in a conduction heat transfer model of the geometry in question and analyze the corresponding boundary heat fluxes. To that end, a unit step change at one of the surfaces needs to be applied while the other boundary temperatures are held at zero. This needs to be repeated for each boundary. The transient admittive and transmittive fluxes resulting from applying a step change to the boundary temperature of one pipe are illustrated in Fig. 2.

These admittive and transmittive fluxes determined from step response calculations are used to derive the weighting factors. To arrive at a discrete formulation, Claesson [46] showed that the exact discrete weighting factors can be calculated from the differences in piece-wise step response fluxes averaged over each time step (size Δt, index m) [46] as follows:

$$\kappa_{ia,m} = \frac{-1}{K_i}\frac{dQ_{ia}(\tau)}{d\tau} \cong \frac{\bar{Q}_{ia}(m\Delta t - \Delta t) - \bar{Q}_{ia}(m\Delta t)}{\bar{K}_i}$$
$$\kappa_{ij,m} = \frac{-1}{K_{ij}}\frac{dQ_{ij}(\tau)}{d\tau} \cong \frac{\bar{Q}_{ij}(m\Delta t - \Delta t) - \bar{Q}_{ij}(m\Delta t)}{K_{ij}} \quad (9)$$

In practice, when using a numerical model to calculate the step response fluxes, this simply means the boundary fluxes calculated from current and previous time steps are used to calculate each weighting factor in the series of weighting factors. This is a straightforward process that needs to be carried out once and the weighting factors stored for subsequent simulations of the model.

The average temperature boundary at the current time step (n) in the DTN representation can be calculated from the summation of boundary temperature sequences (defined by a discrete time series, index q) multiplied by the respective weighting factors:

$$\bar{T}_{ia,n} = \sum_{q=1}^{\infty} \kappa_{ia,q} \cdot T_{i,n-q} \quad (10)$$

$$\bar{T}_{ij,n} = \sum_{q=0}^{\infty} \kappa_{ij,q} \cdot T_{i,n-q} \quad (11)$$

The calculation of ground heat transfer during simulation becomes a process of updating the weighted temperatures at each step and calculating the fluxes using the algebraic equations, Eq. (8). Once the weighting factors are found, the simulation calculation is computationally very efficient but as accurate as the underlying method used to calculate the weighting factors.

2.2. Boundary conditions

In the DTN method, the step response heat flux data is calculated based on the assumption that surface heat transfer coefficients (h) are constant. However, in complex cases with variable boundary conditions, a more effective approach needs to be implemented. The approach taken in this research is to define a boundary temperature, i.e. "effective temperature" (T_e), that where applied by using the predefined constant heat transfer coefficient, gives the expected surface heat flux as applying a more complex boundary condition model. In other words, the effective temperature, or environmental temperature, does not correspond directly to a physical boundary temperature but is applied in the DTN heat balance equations and when the weighted average temperature is updated. This concept has been successfully implemented in DTN modeling of other ground-coupled energy systems [47–49]. In this research, the approach is applied to all boundary conditions in the district heating pipe system: at the ground surface and the supply and return pipe surface.

One of the advantages of the DTN approach defined with three active surfaces is that the model can effectively deal with the environmental conditions that vary at the ground surface (e.g., solar radiation and wind speed) and so the model can be sensitive to climatic conditions at the location of the system. The ground surface heat balance is dealt with by calculating and updating the heat transfer coefficients for each time step using well-known correlations and environmental data that are simply read from a file at each time step.

Due to the significant role of the heat flux at the pipe surface in the driving of the network heat balance, the pipe surface's boundary condition requires to be properly defined to relate the pipe boundary temperature with both the inlet and outlet temperature in a three-dimensional DTN representation. The approach used to define the relationship between the fluid temperatures and pipe surface is to make an analogy with an evaporating-condensing heat exchanger for each discretized section of the pipe. Assuming the pipe surface temperature does not vary along the length in question, the buried pipe can be considered a heat exchanger characterized by an effectiveness parameter ϵ, and the Number of Transfer Units NTU. This approach has been used by Strand [54] to modeling pipes in underfloor heating systems and by Rees [40] to model borehole heat exchangers. The relationship between pipe heat balance and the maximum possible temperature difference between an inlet and pipe surface can be defined as follows:

$$Q_p(t) = \epsilon \dot{m} C_f (T_{\text{in}}(t) - T_{\text{p}}(t)) = \dot{m} C_f (T_{\text{in}}(t) - T_{\text{out}}(t)) \quad (12)$$

The effectiveness (ϵ) can be calculated based on the Number of Transfer Units ($NTU = (2\pi r_p L h_f)/(\dot{m} C_f)$), as follows:

$$\epsilon = 1 - e^{-NTU} \quad (13)$$

The pipe surface heat transfer coefficient (h_f) is calculated using the well-known Gnielinski's correlation, owing to the wide validity range, i.e. for Re numbers between 3×10^3 and 5×10^6, which is practical for the typical range for buried pipe applications. The Gnielinski's correlation can be expressed as follows [55]:

$$h_f = \frac{\lambda_f (f/8)(Re - 1000)Pr}{2r_p \left[1 + 12.7(f/8)^{1/2}\left(Pr^{2/3} - 1\right)\right]} \tag{14}$$

where f and Pr are the Darcy friction factor, and the Prandtl number (ratio of momentum diffusivity to thermal diffusivity), respectively. Assuming the copper pipe as a smooth pipe, the friction factor can be estimated as

$$f = (0.79ln(Re) - 1.64)^{-2} \tag{15}$$

It is possible, by rearranging the DTN heat balance equations for the pipe surfaces to calculate the effective pipe boundary temperatures in a way that avoids iteration using only the inlet temperature (T_{in}) as the time-varying input data. The temperature that needs to be defined in the DTN heat balance equation for one of the pipes (taking the supply pipe as surface 2 for example here) T_2 at a given time step. An instantaneous heat balance can be defined at the pipe surface by equating Q_p (Eq. (12)) with the convective flux at the surface (dropping t for simplicity) with temperature T_p as follows,

$$\varepsilon\, \dot{m} C_f \left(T_{in} - T_p\right) - h_f A_2 (T_2 - T_p) = 0 \tag{16}$$

A further heat balance can be defined using the DTN heat balance equation for surface 2 (Q_2 in Eq. (8)) and the convective flux at the pipe surface,

$$K_2 \cdot \left[T_2 - \bar{T}_{2a}\right] + Q_{21} + Q_{23} - h_f A_2 (T_2 - T_p) = 0 \tag{17}$$

The term with $\bar{T}_{2a}$ is based on past temperatures and so is known at the start of any time step. As the transmittive fluxes change very slowly, these can also be taken as the most recent values. These can also be grouped into a term $\bar{Q}$ representing historical fluxes so that the heat balance can be abbreviated as

$$K_2 \cdot T_1 + \bar{Q} - h_f A_2 (T_2 - T_p) = 0 \tag{18}$$

This can be rearranged to find an expression for T_p,

$$T_p = T_2 - \frac{K_2 \cdot T_2 + \bar{Q}}{h_f A_2} \tag{19}$$

This can be substituted in Eq. (16) to eliminate T_p. This gives an expression for T_2 that only involves the inlet temperature and historical heat fluxes as follows:

$$T_2 = \left(T_{in} - \bar{Q}/h_f A_2\right) / \left(1 - \frac{K_2}{h_f A_2} + \frac{K_2}{\varepsilon \dot{m} C_f}\right) \tag{20}$$

This temperature is then used in the solution of the DTN heat balance equations (Eq. (3)) to find the respective fluxes. The pipe flux is equivalent to Q_2 in the case of the supply pipe i.e. $Q_p = Q_2$, so that the outlet temperature can be found from the heat balance on the fluid (Eq. (16)):

$$T_{out}(t) = T_{in}(t) - \frac{Q_p}{\dot{m} C_f} \tag{21}$$

The same procedure is followed for surface 3 in the case of the return pipe. The same approach has been adopted to relate the pipe boundary conditions with the inlet and outlet temperatures in the DTN method and has been validated for application to modeling of diaphragm wall ground heat exchangers [49] and energy pile [47].

2.3. Modeling fluid responses

The heat transfer fluid flow and its short timescale dynamic effects in the district heating pipelines can be represented by a one-dimensional convection–diffusion model as follows [36,37,42],

$$\frac{\partial T(x,t)}{\partial t} + \upsilon \frac{\partial T(x,t)}{\partial x} - D \frac{\partial^2 T(x,t)}{\partial x^2} = 0 \tag{22}$$

where υ is the longitudinal velocity and D is the diffusion coefficient which depends on the velocity profile and Reynolds number. For the calculation of diffusion coefficient (D) an empirical relation [36] in terms of Peclet Number, Pe (the ratio of advective transport rate to the diffusive transport rate) can be applied as follows,

$$\frac{D}{L\upsilon} = \frac{1}{Pe} = \frac{2r_p}{L}\left(3 \times 10^7 Re^{-2.1} + 1.35 Re^{-0.125}\right) \tag{23}$$

The exact solution of Eq. (22) can be found in the Laplace domain. However, these are only useful for modeling constant flow rates.

Due to this fact, a number of discrete approximations have been proposed in the literature. One approximation to the convection–diffusion formulation (Eq. Eq. (22)) is conceived as a combination of the plug flow with diffusion represented by discretization using a variable number (N) of continuously stirred tanks (denoted as the PFST model). In this model, the transit time for fluid flow through a pipe is determined by the ratio of the pipe length (L) to the mean fluid velocity (υ), expressed as ($\tau = L/\upsilon$). This transit time (τ) can be divided between transit through two components: the first component is associated with the transport time delay (τ_0), while the remaining time is dedicated to the N stirred tank elements ($N\tau_N = \tau - \tau_0$) as illustrated in Fig. 4. Skoglund et al. [37,56] demonstrated that τ_N can be calculated by Eq. (24) with very good agreement with the convection–diffusion model (Eq. (22)).

$$\tau_N = \sqrt{\frac{2LD}{N\upsilon^3}} = \tau\sqrt{\frac{2}{NPe}} \tag{24}$$

Using Eq. (24), τ_N and τ_0 can be determined for a given number of tanks, and as a result, the length (L_N) and volume of each tank can be calculated. There is some freedom to choose the number of tanks in the discretization but beyond this range there is no benefit in increasing the number of tanks. For practical purposes, a preferred number of tanks can be estimated using a linear correlation, expressed as ($N = 0.04Pe - 5.34$). The validity of this approximation has been demonstrated across a range of Reynolds numbers and pipeline geometries, particularly in situations involving heat transfer [42]. The PFST model is shown to be able to accurately capture the dynamic short-timescale effects of fluid flow in very good agreement with the experimental data as we have elaborated elsewhere [42]. Coupling of this model with a finite volume heat transfer model has also been demonstrated elsewhere [40].

2.4. Weighting factor derivation

Weighting factors series can be derived from analyses of the transient heat fluxes resulting from applying a step boundary condition to each surface in turn. In this research, the weighting factors are extracted from such responses calculated using a detailed numerical model. Based on the design parameter of the district heating pipeline system such as pipeline diameter and depth, insulation dimensions and the total length of the buried pipeline, the geometry of the system has been generated, meshed, and solved using the OpenFOAM finite volume method (FVM) library [57]. The details of the FVM model including mesh generation and discretization schemes used to solve the governing equations are described and explained in the related thesis [18]. In principle, using a numerical model to derive the weighting factors allows heterogeneous thermal properties (e.g., different combinations of ground materials near the pipe trench) to be accounted for.

Having calculated three sets of step response data in the form of heat flux time series, as shown in Fig. 2, admittive and transmittive weighting factor series (six sets in total) are determined for the desired time step size using Eq. (9). More details of this process can be found in studies by Wentzel [51] and Rees and Fan [48]. Example transmittive and admittive weighting factor series for heat fluxes in a buried one-pipe pipeline system are shown in Fig. 3.

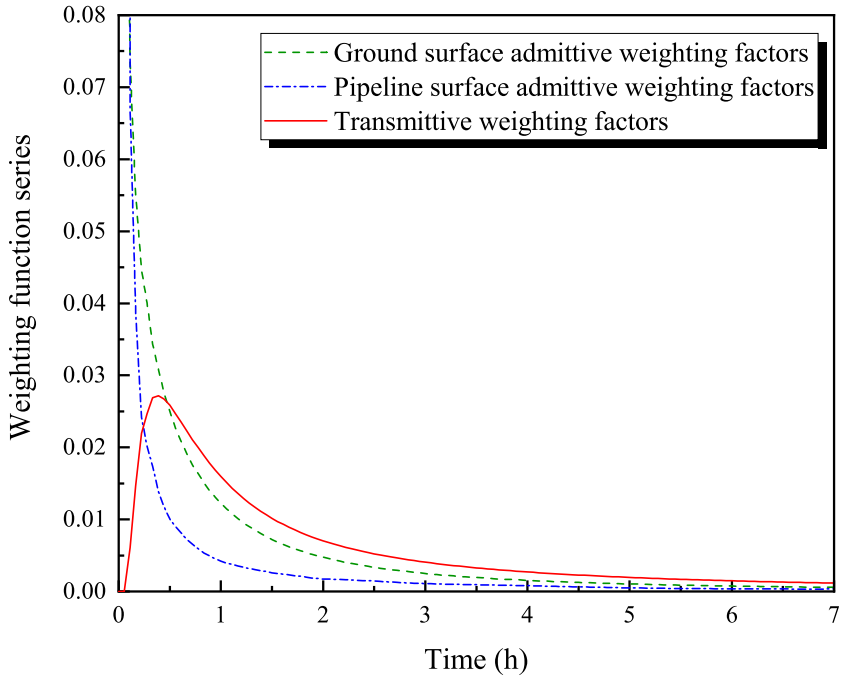

Fig. 3. An example of transmittive and admittive weighting factor series for a buried pipeline system.

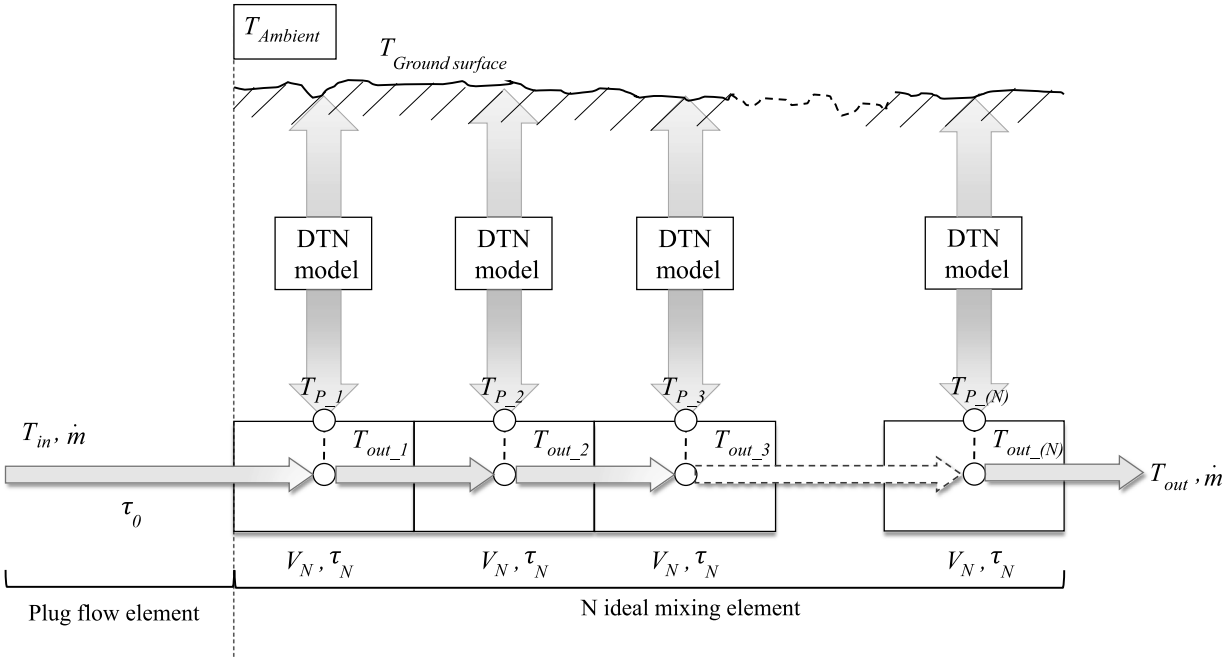

Fig. 4. A diagram of the combined dynamic thermal network (DTN) method with the discretized heat transfer fluid flow model through a pipeline, i.e. the PFST model.

2.5. Combined DTN-PFST model

The aim has been to develop a model that represents the dynamic thermal behavior of buried pipelines such as those in district heating, considering the transient ground heat transfer over a wide range of timescales as well as longitudinal transport phenomenon. The DTN model allows representation of the ground heat transfer and the PFST model represents the longitudinal transport of the fluid, including its thermal capacity, to be represented. The DTN model is two-dimensional in a vertical plane (pipe and trench cross-section) and the PFST model is one-dimensional in the longitudinal direction. If the pipeline is relatively short then the assumption that the ground/pipe interface temperature is constant over this section is reasonable and it is possible to couple the PFST model with one instance of the DTN model. However, for more realistic long pipelines, it is necessary to discretize the system further and use multiple instances of the DTN model to capture the variation in ground temperatures over the length of the pipeline. Combining the two types of model in this way then results in a quasi-three-dimensional representation. The configuration of the combined DTN-PFST model is illustrated in Fig. 4.

Where the two models are combined and the DTN model is coupled to a given 'tank' of the PFST model, Eq. (21) is solved where T_{in} is taken to be T_{out} from the upstream tank and T_{out} is the temperature of the stirred tank in each case as indicated in Fig. 4.

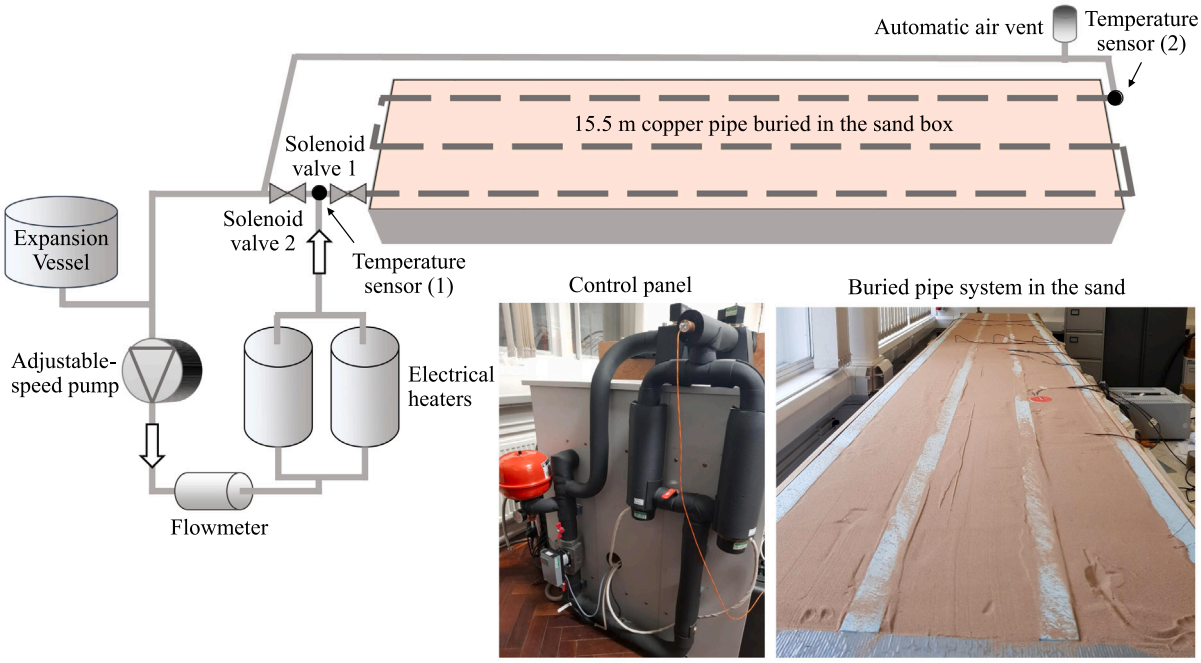

Fig. 5. A schematic of the experimental facilities and photographs of the buried pipe section and fluid circulation system.

In many situations, it would be sufficient to precalculate the DTN weighting factors for a given pipe size and set of ground conditions and use the same data for each instance of the coupled DTN model. However, there is flexibility in the way that weighting factors and ground boundary conditions are applied along the length of the pipeline. Hence variations in ground conditions (e.g. soil properties) and surface conditions (e.g., changes between tarmac, concrete and grass-covered surfaces) can be dealt with.

It should be noted that the PFST model is not noticeably sensitive to the choice of the number of tanks. Therefore, changes in flow rate within the practical ranges of interest do not result in a significant error in the calculation of the pipeline outlet temperature [42].

2.6. The modeling process

In the DTN-PFST simulation process, prediction of heat transfer rates and fluid temperatures is carried out for the given inlet temperature and flow rate, as well as environmental conditions at each time step for a given element. In this relatively computationally simple process, the heat balance equations (Eq. (8)) are solved based on the derived weighting factor series and the input data at each time step.

The application of the combined DTN-PFST model proposed in this research consists of three main processes: step response flux calculations, weighting factors derivation, and model simulation process. In general, since the step response flux calculation is required to be analyzed only once for a given pipe cross-sectional geometry and set of thermal properties, the heat flux series can be stored and used in multiple simulations. The simulation steps of the combined DTN-PFST model can be summarized as follows:

1. Determine the step response heat flux data for each pipe and ground geometry and thermal properties.
2. Calculate the optimal number of elements based on the Pe number of fluid flow using the PFST model calculation and divide the system in the axial direction accordingly.
3. Analysis of the step response data for each configuration to calculate and store the weighting factor series.
4. At the start of each system simulation, read the weighting factor files and initialize the temperatures for each section.
5. Calculate surface heat fluxes using time-varying boundary inlet and environmental conditions for each section.
6. Update the weighted average temperature data series.
7. Calculate total heat transfer rates and outlet temperatures.

Steps 1–3 require the most computational effort but are pre-calculated prior to the simulation and stored as necessary. Steps 4–7 are repeated over the simulation time step series. Since the heat balance equations are simple algebraic expressions and the only other requirement in the simulation stage is to update the temperature histories, simulations with long time series data can be dealt with very efficiently. The accuracy and computational cost of the proposed model are further compared with that of a detailed 3D model and experimental data in modeling the long buried pipelines in Section 4.

3. Experimental design

In this research, a scaled-down district heating system pipeline was designed and built to validate the combined DTN-PFST model with experimental data obtained under a range of controlled conditions. The main experimental challenges are the implementation of step changes to the thermal and fluid flow boundary conditions. The test apparatus consists of two pressurized hydraulic circuits separated by solenoid valves. One circuit represents the buried pipe section (right-hand circuit) and another represents a heat source (left-hand circuit). The main components of the heat source circuit are shown schematically and illustrated in Fig. 5. Two fast-response PT100 sensors (accuracy 1/10 DIN) are directly inserted into the buried pipe used to measure the inlet and outlet temperatures of the test pipe section which is a 15.5 m buried pipe with the inner and outer diameters of 13.6 and 15 mm, respectively. The pipe is buried in the dry sand of known thermal properties and with the sides and bottom insulated to limit parasitic heat losses. The ambient temperature is measured with type *T* thermocouples and laboratory conditions are continuously monitored. All temperature sensors are calibrated using a calibration oil bath and a reference RTD (Resistance Temperature Detector) so that the uncertainty in the temperature measurements of the thermocouples and pt-100 sensors has been estimated to be 0.167 K and 0.062 K, respectively. A variable-speed pump and flowmeter are used to control

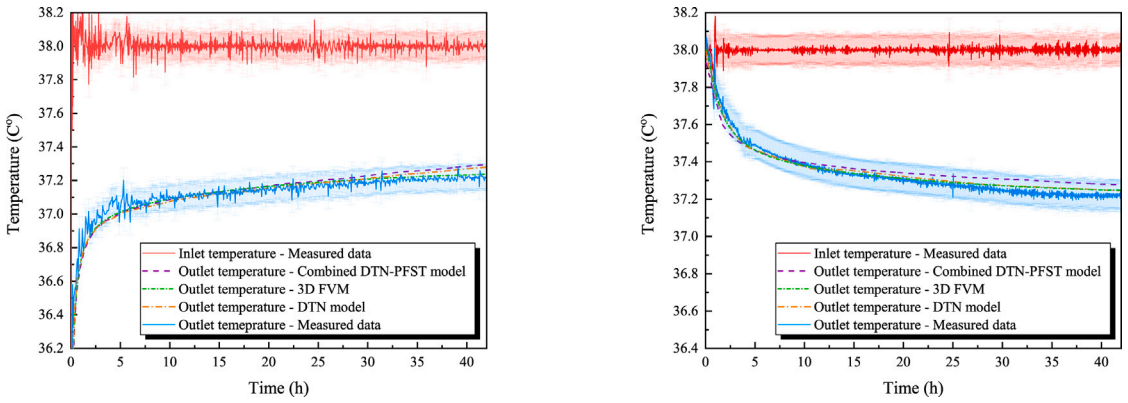

Fig. 6. Measured and predicted outlet temperatures by the numerical models for the experiment (left) the step change to the buried pipe (right) the step change to the ground surface.

the flow rate and vary this between experiments as required. The experimental flow conditions need careful consideration as the fluid flow conditions need to be turbulent and constant to represent the constant convection coefficient conditions assumed in weighting factors derivation. At the same time, the flow rate has to be limited to ensure a total temperature difference large enough relative to the uncertainty in the temperature measurements to derive the overall heat transfer rates.

The measurement of heat flux at the ground surface is carried out through direct measurement of flux obtained using three self-calibrating heat flux sensors (HFP01SC by Hukseflux). These self-calibrating heat flux sensors have been placed on the top of the sandboxes allowing for the accurate measurement of the dynamic ground surface heat losses.

This experimental facility was also used for evaluating the short time-scale dynamic behavior of the pipe alone (without using sand) with a focus on the effects of the longitudinal dispersion of fluid flow on shaping the temperature profile. Details of the operating conditions and experimental results are presented elsewhere [42] and demonstrate the validation of the PFST model used with insulated and noninsulated pipes. Here, we focus on the validation of the DTN calculations of ground heat transfer and the coupled model.

Imposing the step change in fluid temperature boundary conditions is carried out by circulating water in the heat source circuit to be preheated by the electric heaters, while the buried pipe section is isolated and stabilized at ambient room temperature. When conditions are stabilized, the step change in the inlet temperature is applied by opening the solenoid valve between the two circuits such that the hot water flows through the buried pipe at the set inlet temperature. A closed-loop feedback controller is used to modulate heat input in order to keep the inlet temperature constant. The inlet and outlet temperatures of the buried pipe section are recorded at the given time step during the experiments until the steady-state conditions are approached: almost 42 h.

In addition to the step change to the pipeline, a step change to the ground surface is applied. For that purpose, the sand and pipe section is first preheated until the section reaches a uniform initial temperature above the laboratory ambient temperature. This is accomplished by using the pipe as a heater but adding additional insulation (a combination of flexible foam insulation fixed to rigid foam insulation) to the top of the sand temporarily to enable isothermal conditions to be achieved. A step change is then initiated by rapidly removing the upper insulation and immediately exposing the upper surface to ambient conditions. Rapidly removing the upper insulation allows the reversed step change to start and data is recorded until steady conditions are approached.

4. Model validation

The validity of the combined DTN-PFST model has been evaluated by making comparisons with experimental district heating pipeline data over a range of time and spatial scales. The comparison between the proposed model, the singular DTN model and the detailed three-dimensional finite volume model has been also made to assess their accuracy and relative computational costs. Experimental data have been obtained from two district heating pipeline systems: (i) the lab-scale district heating system (as described in Section 3) and, (ii) a single pipe section in the Vilnius district heating system (detailed in the Ref. [58]. Data from the latter system has been used in other validation studies [17,59]) for evaluating the ability of proposed models to reproduce district heating pipeline dynamic thermal responses.

4.1. Outlet temperature prediction: lab-scale DH pipeline

The evaluation of dynamic thermal responses of district heating pipelines has firstly been conducted by performing a temperature step change test using the lab-scale pipeline system described in Section 3. The step changes are chosen to mimic the step response assumed in deriving all DTN weighting factors, i.e. a step change in boundary temperature (fluid or surrounding air in these cases) with the other surface maintained at the initial temperature of the system. Having prepared the system and making sure the buried pipe and surrounding sand of the system is at a stable temperature (21.8 °C), the water was pre-heated in the heat source circuit via the immersed heater and controlled to reach a steady temperature of 38 °C. This fluid was then introduced to the buried pipe section to initiate the step change and subsequently, the inlet temperature and fluid flow rate were maintained constant (38 °C, 0.246 m/s, Re = 4900 respectively) and the outlet temperature and the ground surface heat fluxes were measured and recorded until the system approached steady-state conditions (almost 42 h).

In order to gather the corresponding step response data at the ground surface, a further experiment was performed. Application of the step change in temperature at the ground surface was achieved in an inverted sense with the ground boundary condition cooler than the initial temperature (effectively a step from 0 to −1 rather than 0 to 1) with the fluxes being of the same magnitude but opposite sign. This was achieved by elevating the buried pipe and sand above the ambient laboratory temperature. This required the ground surface to be temporarily insulated by adding further rigid sheet insulation as described at the end of Section 3. Having pre-heated the sand and pipe section (including the sand at the surface) to achieve a uniform initial temperature of 38 °C the surface insulation was rapidly removed to expose the surface to the cooler lab environment to initiate the step change in conditions. The pipe boundary conditions were kept constant at an inlet temperature of 38 °C and constant velocity of 0.273 m/s (Re = 5450). The outlet temperature and the ground surface heat fluxes were measured and recorded until the steady-state conditions were approached.

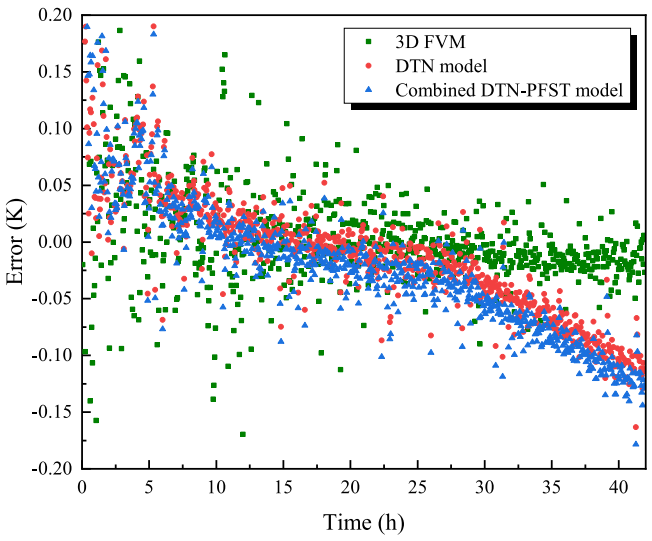

Fig. 7. Error between the measured outlet temperature and the predicted values by the numerical models for the experiment imposing a step change to the buried pipe temperature.

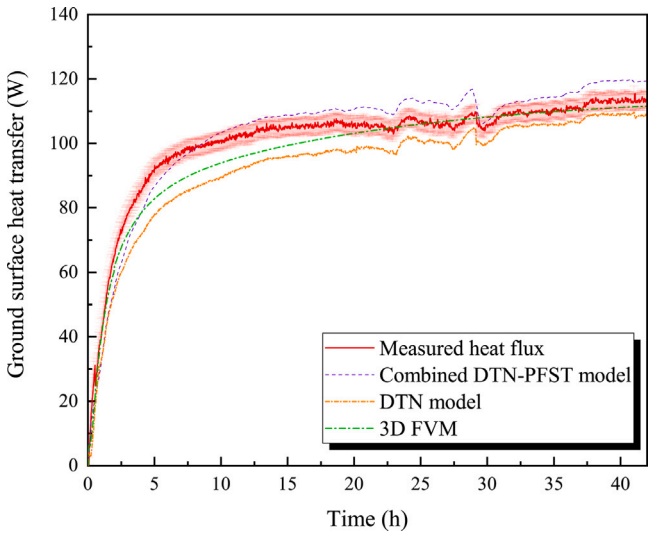

Fig. 8. Measured and calculated ground surface heat transfer for the case of the step change to the buried pipe.

The variation in predicted outlet temperatures is compared with measured values during both experiments in Fig. 6. The general trend of the pipeline temperature predictions by the numerical models can be seen to be in good agreement with the measurement data in both sets of experimental conditions. The magnitude of the discrepancies between the measured and predicted outlet temperatures by the numerical models for the case of a step change to the pipeline are also shown: Fig. 7. The difference between the outlet temperatures predicted by the combined DTN-PFST model falls mostly within the range of the experimental temperature measurement error, which is estimated to be 0.07 K in magnitude. The data outside this range are at times corresponding to the initial change in conditions where the heat controller action needs to be at its greatest and control is less than ideal — the temperature being very stable thereafter.

Fig. 8 shows a comparison between the ground surface heat transfer rates predicted by the numerical models and the measured values when a step change is applied to the pipeline inlet temperature. It can be observed the difference between the predicted and measured ground heat fluxes are generally small, and as time progresses, the differences reduce further for all models, with final differences being less than 5% in magnitude. Some particular fluctuations are apparent between 22 and 30 h which are due to the small variations in the lab conditions (A maximum variation of 0.9 K in lab temperature was observed over the whole data collection period). These fluctuations do not notably affect the overall ground heat transfer, yet even these small fluctuations in lab temperature can be seen reflected in the outcome of the DTN models, due to the fact that DTN models are driven by time-varying boundary conditions.

Table 1 presents the comparisons between the Root Mean Square Error (RMSE) between the measured and predicted outlet temperature using the numerical models throughout the test period, that is, 42 h. The results demonstrate that the combined DTN-PFST model is capable of predicting the outlet temperature with an acceptable level of accuracy. The model predictions are of the same level of accuracy as the detailed 3D model while being more than almost five orders of magnitudes more computationally efficient. This level of accuracy, along with computational efficiency, makes the model well suited to represent district heating pipelines and related short-timescale dynamic thermal effects. Further details of this validation exercise have been published elsewhere [60].

Table 1
Comparison between the RMSE and calculation time required for the numerical models.

Model	RMSE (K)	Calculation time
3D FVM	0.121	82.3 h
DTN model	0.078	4.6 s
Combined DTN-PFST model	0.076	6.7 s

4.2. Outlet temperature prediction: full-scale DH pipeline

The validity of the combined DTN-PFST model in modeling the operational district heating pipeline under real operating conditions has been evaluated using experimental data available from an operational district heating pipeline in Vilnius [58]. Temperature measurements were obtained from the thermistors at each end of a preinsulated pipe section of length 470 m with a nominal diameter of 300 mm. The flow velocity was 0.27 m/s corresponding to $Re = 3 \times 10^4$ which is at the lower end of the range expected in district heating systems but representative of low demand conditions. In the experiment, a heat pulse was introduced at the inlet of the system by raising the temperature by approximately 5 K.

Fig. 9 illustrates the comparisons between the simulation results of the proposed model and the measurement data. The differences between the values of the outlet temperature compared to the inlet are illustrative of the heat losses over the pipe. The delay between the initiation of the heat pulse and the response at the outlet is more than 3 h. The general trend of the pipeline outlet temperature predicted by the model can be seen to be in good agreement with the monitoring data both in terms of temperature and time displacement. The maximum temperature at the outlet is over-predicted by a maximum of 0.93 °C which is a difference larger than the reported experimental uncertainty of ±0.3 K.

Validation studies using other modeling approaches have also reported an over-prediction of the peak temperature in comparison with this Vilnius experiment [58]. The results from the proposed model are compared with the outlet temperatures predicted by two other models in Fig. 10. These are a Finite Element Model [59] and an improved plug flow model [17]. This comparison suggests that the proposed model performs well relative to other models. Other authors of the original study have suggested that at such relatively low velocities, the results may be sensitive to convection conditions (correlations) [17] and possibly stratification in the pipe affecting the measurements [61].

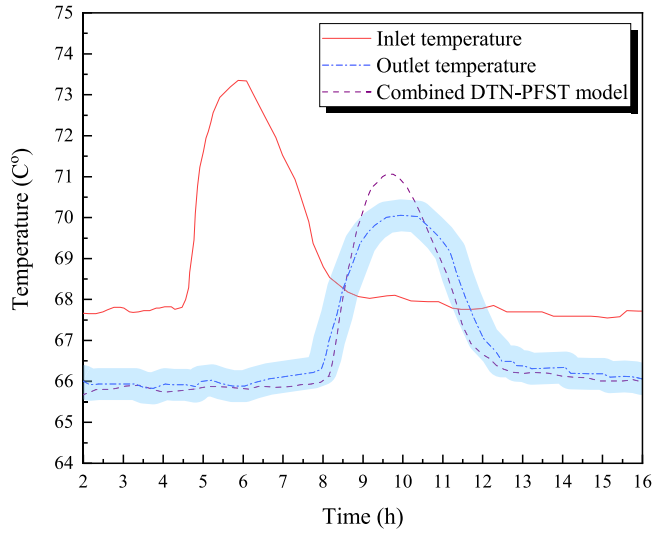

Fig. 9. Predicted outlet temperature response using the combined DTN-PFST model and monitoring data with the tolerance from the Vilnius district heating pipeline.

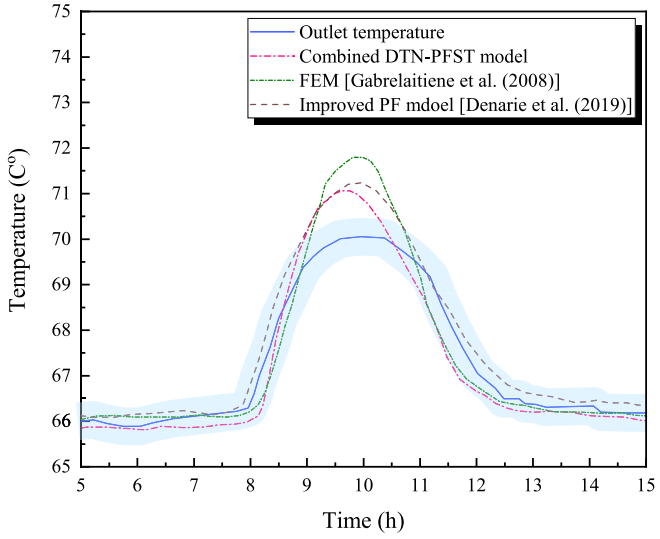

Fig. 10. Comparisons between the simulation results obtained from the combined DTN-PFST model and two other numerical models [17,59] in predicting the outlet temperature response of the Vilnius district heating pipeline.

It should be noted that in the two other numerical models, the dynamic heat transfer in the surrounding ground has not been considered, and merely a steady-state thermal resistance has been used between the fluid, pipeline, and the ground. This simplification does not appear to have a major impact on the prediction of temperature in the Vilnius district heating pipeline experiment, as the pipeline was insulated, and therefore the heat transfer from the fluid flow to the ground was small and changed negligibly during the monitoring period.

5. Modeling of pipeline heat storage

An objective in developing the model was to be able to evaluate the dynamic storage of thermal energy when, for example, the temperatures of the heat source are temporarily elevated. To demonstrate the ability of the proposed model in this regard, a relatively long buried pipeline has been modeled using a similar geometry of the test rig, but 100 m long. The same cross-sectional geometry is used so that there is correspondence with that used in model validation and derivation of

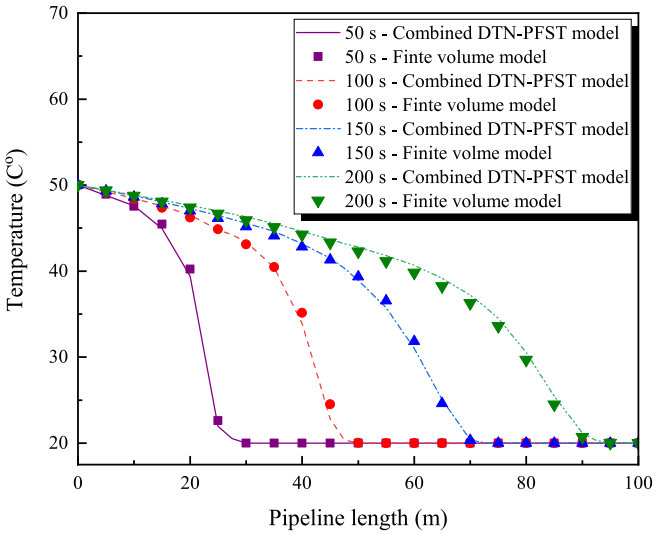

Fig. 11. Variations of the fluid temperature along the 100 m pipeline calculated by the combined DTN-PFST model at four different times.

the weighing factors. The DTN-PFST model was accordingly developed using weighting factors derived from step responses calculated by the detailed 3D model (Finite Volume Method), but with additional instances of the pipe elements and coupled DTN representation of the ground (as illustrated in Fig. 4). In this case, turbulent fluid flow with a velocity of 0.5 m/s (Re = 10,377) has been modeled with initial thermal conditions of 20 °C. A step change of 30 K is applied to the pipeline inlet temperature so that this is maintained at 50 °C for the duration of the test i.e., 1000 s. As the fluid progresses through the pipeline, the energy contained in the pipeline and transferred to the ground increases. Variations in fluid temperature along with the buried pipeline obtained from the combined DTN-PFST model and the 3D model are shown in Fig. 11. It can be observed that the combined DTN-PFST model is able to predict the variation of the fluid temperature along the buried pipeline in very good agreement with the detailed 3D model. The DTN-PFST is furthermore more than five orders of magnitude faster than the 3D numerical model.

The variations of the outlet temperature responses calculated by the model at six locations along the pipeline are shown in Fig. 12. It can be seen that for longer distances, the temperature responses become more diffused such that the rate of increase of temperature is slower. This reflects a combination of plug flow and longitudinal dispersion. The fact that the temperatures approach lower values on longer timescales (700 s in this case) also reflects heat loss along the pipe. Heat is progressively stored along the pipe as cold fluid is flushed through. Heat losses are present and increase as the warm fluid progresses along the pipe. Thus, the value of combining both the DTN and PFST models is demonstrated. This simulation illustrates that it is possible to use the combined model to study questions of how much energy is stored in the pipeline network and how much energy at a particular temperature can be delivered to the end-users of the network at particular times.

Fig. 13 shows the variations of the cumulative energy stored in the fluid in the pipeline with respect to the initial temperature over the length of the pipeline. The corresponding energy stored in the pipeline fluid is calculated from predicted fluid temperature variations at each discrete section of the model. The cumulative energy stored along the pipeline can be obtained from the sum of the change in energy stored in each section ($\Sigma M_i C_p \Delta T_i$). The energy stored as fluid is transported along the pipeline is shown at different times in Fig. 13.

It can be seen that with the increase in the distance from the inlet of the pipeline, the energy storage of the pipeline increases: up to 1400 KJ for the entire length of the pipeline after 250 s. Being able to calculate

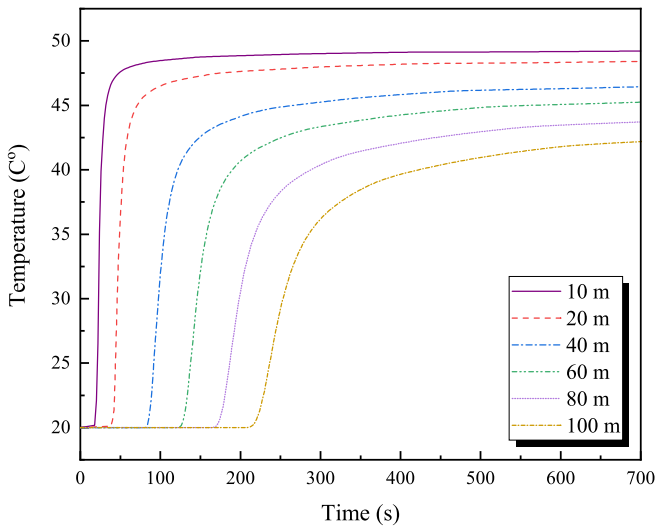

Fig. 12. Predicted temperature responses of the pipeline at six different distances calculated by the combined DTN-PFST model.

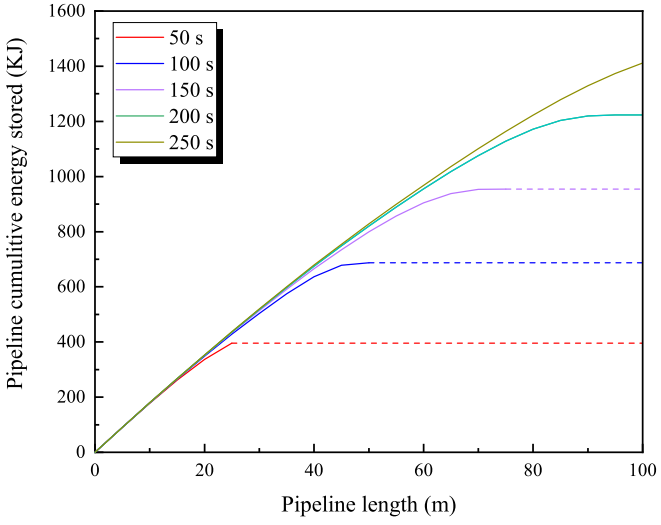

Fig. 13. Variations of the energy stored at five times over the length of the buried pipeline. The solid portions of the lines indicate the extent of progression of warm fluid at each time.

such variations may be particularly important in studying the effects of variations in source temperature on energy storage and the dynamic effect on return temperatures experienced at the heat source in real systems with much larger pipe sizes and lengths.

The energy stored does not increase linearly over time as ground heat losses also increase as warm fluid progresses along the pipeline. This effect would be relatively smaller in larger diameter pipes that are well insulated. In applications other than high-temperature district heating such as ambient temperature networks or geothermal heat exchangers (uninsulated plastic pipes), the DTN element of the combined model also brings the benefit of being able to calculate seasonal variations in ground thermal conditions and corresponding variations in heat losses and ground energy storage.

6. Conclusions

A novel buried pipe model has been introduced combining a discretized one-dimensional fluid flow model and the Dynamic Thermal Network conduction heat transfer model denoted a DTN-PFST model. The model is capable of predicting the dynamic thermal behavior of buried pipeline systems under a range of operating conditions. This combination enables the proposed model to take advantage of the features of the DTN method to model transient ground conduction. These advantages include the ability to efficiently represent complex geometries and heterogeneous thermal properties such as those found in pairs of heat network pipes and varieties of trench fill and surface materials. It is also advantageous in being able to deal with a very long time series input such as seasonal climate-driven loads and environmental conditions in a highly computationally efficient manner. The second element of the model is a longitudinal fluid transport model, called the combined plug flow N-continuously stirred tanks (PFST model) which is used to capture short-term dynamic effects and the heat capacity of the pipe fluid.

Validation of the proposed DTN-PFST model has been conducted using experimental data from both lab-scale and full-scale district heating pipelines. The simulation results from a 3D conjugate heat transfer model are also used to compare with the proposed models outcomes in terms of the computational cost and accuracy. The results of these validation studies have shown that the combined DTN-PFST model is not only able to accurately simulate the dynamic behavior of the buried pipeline system in very good agreement with the experimental data, but also in a significantly more computationally efficient manner: more than five orders of magnitude quicker. The ability of the model to represent the temperature propagation through the pipeline along with transient ground heat transfer conditions in a very computationally efficient manner makes the model appealing for routine dynamic thermal analysis and design tasks of current and future thermal energy networks. The model is also well suited to study low-temperature buried pipe systems such as water/wastewater pipelines, horizontal ground heat exchangers and ground energy storage applications.

CRediT authorship contribution statement

Saleh S. Meibodi: Data curation, Formal analysis, Investigation, Methodology, Software, Validation, Visualization, Writing – original draft. **Simon Rees:** Conceptualization, Funding acquisition, Investigation, Methodology, Project administration, Resources, Software, Supervision, Writing – review & editing. **Fleur Loveridge:** Funding acquisition, Project administration, Resources, Supervision, Writing – review & editing.

Declaration of competing interest

The authors declare the following financial interests/personal relationships which may be considered as potential competing interests: Saleh S Meibodi reports financial support was provided by UK Research and Innovation.

Data availability

The data associated with this paper are openly available from the University of Leeds Data Repository: https://doi.org/10.5518/1439.

Acknowledgments

This work was supported by the University of Leeds, United Kingdom through a doctoral scholarship; and the Engineering and Physical Sciences Research Council (EPSRC), United Kingdom project "Integrated Infrastructures for Sustainable Thermal Energy Provision" (grant reference EP/S001417/1).

References

[1] Mi P, Zhang J, Han Y, Guo X. Study on energy efficiency and economic performance of district heating system of energy saving reconstruction with photovoltaic thermal heat pump. Energy Convers Manage 2021;247:114677. http://dx.doi.org/10.1016/j.enconman.2021.114677.

[2] Østergaard DS, Smith KM, Tunzi M, Svendsen S. Low-temperature operation of heating systems to enable 4th generation district heating: A review. Energy 2022;248:123529. http://dx.doi.org/10.1016/j.energy.2022.123529.

[3] Lake A, Rezaie B, Beyerlein S. Review of district heating and cooling systems for a sustainable future. Renew Sustain Energy Rev 2017;67:417–25. http://dx.doi.org/10.1016/j.rser.2016.09.061.

[4] Mazhar AR, Liu S, Shukla A. A state of art review on the district heating systems. Renew Sustain Energy Rev 2018;96:420–39. http://dx.doi.org/10.1016/j.rser.2018.08.005.

[5] van der Heijde B, Vandermeulen A, Salenbien R, Helsen L. Representative days selection for district energy system optimisation: a solar district heating system with seasonal storage. Appl Energy 2019;248:79–94. http://dx.doi.org/10.1016/j.apenergy.2019.04.030.

[6] Ozgener L, Hepbasli A, Dincer I. A key review on performance improvement aspects of geothermal district heating systems and applications. Renew Sustain Energy Rev 2007;11(8):1675–97. http://dx.doi.org/10.1016/j.rser.2006.03.006.

[7] Verda V, Guelpa E. District heating network modelling for the analysis of low-exergy sources. ASME international mechanical engineering congress and exposition, Vol. 6 (Energy), 2017, http://dx.doi.org/10.1115/IMECE2017-72390.

[8] Bühler F, Petrović S, Karlsson K, Elmegaard B. Industrial excess heat for district heating in Denmark. Appl Energy 2017;205:991–1001. http://dx.doi.org/10.1016/j.apenergy.2017.08.032.

[9] Ommen T, Thorsen JE, Markussen WB, Elmegaard B. Performance of ultra low temperature district heating systems with utility plant and booster heat pumps. Energy 2017;137:544–55. http://dx.doi.org/10.1016/j.energy.2017.05.165.

[10] Buffa S, Cozzini M, D'Antoni M, Baratieri M, Fedrizzi R. 5Th generation district heating and cooling systems: A review of existing cases in {*Europe*}. Renew Sustain Energy Rev 2019;104:504–22. http://dx.doi.org/10.1016/j.rser.2018.12.059.

[11] Meibodi SS, Loveridge F. The future role of energy geostructures in fifth generation district heating and cooling networks. Energy 2022;240:122481. http://dx.doi.org/10.1016/j.energy.2021.122481.

[12] Quirosa G, Torres M, Becerra JA, Jiménez-Espadafor FJ, Chacartegui R. Energy analysis of an ultra-low temperature district heating and cooling system with coaxial borehole heat exchangers. Energy 2023;278(January). http://dx.doi.org/10.1016/j.energy.2023.127885.

[13] Li Y, Rezgui Y, Zhu H. Dynamic simulation of heat losses in a district heating system: A case study in {*Wales*}. In: 2016 IEEE smart energy grid engineering (SEGE). 2016, p. 273–7. http://dx.doi.org/10.1109/SEGE.2016.7589537.

[14] Capone M, Guelpa E, Verda V. Accounting for pipeline thermal capacity in district heating simulations. Energy 2021;219:119663. http://dx.doi.org/10.1016/j.energy.2020.119663.

[15] Sartor K, Dewalef P. Experimental validation of heat transport modelling in district heating networks. Energy 2017;137:961–8. http://dx.doi.org/10.1016/j.energy.2017.02.161.

[16] van der Heijde B, Fuchs M, Ribas Tugores C, Schweiger G, Sartor K, Basciotti D, Müller D, Nytsch-Geusen C, Wetter M, Helsen L. Dynamic equation-based thermo-hydraulic pipe model for district heating and cooling systems. Energy Convers Manage 2017;151(August):158–69. http://dx.doi.org/10.1016/j.enconman.2017.08.072.

[17] Dénarié A, Aprile M, Motta M. Heat transmission over long pipes: New model for fast and accurate district heating simulations. Energy 2019;166:267–76. http://dx.doi.org/10.1016/j.energy.2018.09.186.

[18] Meibodi SS. Modelling dynamic thermal responses of pipelines in thermal energy networks (Ph.D. thesis), University of Leeds; 2020.

[19] Keçebaş A, Yabanova I. Thermal monitoring and optimization of geothermal district heating systems using artificial neural network: A case study. Energy Build 2012;50:339–46. http://dx.doi.org/10.1016/j.enbuild.2012.04.002.

[20] Yilmaz C, Koyuncu I. Thermoeconomic modeling and artificial neural network optimization of afyon geothermal power plant. Renew Energy 2021;163:1166–81. http://dx.doi.org/10.1016/j.renene.2020.09.024.

[21] Talebi B, Mirzaei PA, Bastani A, Haghighat F. A review of district heating systems: Modeling and optimization. Front Built Environ 2016;2:1–14. http://dx.doi.org/10.3389/fbuil.2016.00022.

[22] Sarbu I, Mirza M, Crasmareanu E. A review of modelling and optimisation techniques for district heating systems. Int J Energy Res 2019;43(13):6572–98. http://dx.doi.org/10.1002/er.4600.

[23] Guelpa E, Verda V. Thermal energy storage in district heating and cooling systems: A review. Appl Energy 2019;252(June):113474. http://dx.doi.org/10.1016/j.apenergy.2019.113474.

[24] Dalla Rosa A, Li H, Svendsen S. Method for optimal design of pipes for low-energy district heating, with focus on heat losses. Energy 2011;36(5):2407–18. http://dx.doi.org/10.1016/j.energy.2011.01.024.

[25] Danielewicz J, Śniechowska B, Sayegh MA, Fidorów N, Jouhara H. Three-dimensional numerical model of heat losses from district heating network pre-insulated pipes buried in the ground. Energy 2016;108:172–84. http://dx.doi.org/10.1016/j.energy.2015.07.012.

[26] Arabkoohsar A, Khosravi M, Alsagri AS. CFD analysis of triple-pipes for a district heating system with two simultaneous supply temperatures. Int J Heat Mass Transfer 2019;141:432–43. http://dx.doi.org/10.1016/j.ijheatmasstransfer.2019.06.101.

[27] Dalla Rosa A, Li H, Svendsen S. Modeling transient heat transfer in small-size twin pipes for end-user connections to low-energy district heating networks. Heat Transf Eng 2013;34(4):372–84. http://dx.doi.org/10.1080/01457632.2013.717048.

[28] Benonysson A. Dynamic modelling and operational optimization of district heating systems (Ph.D. thesis), Danmarks Tekniske Hoejskole; 1991, p. 234.

[29] Benonysson A, Bøhm B, Ravin HF. Operational optimization in a district heating system. Energy Convers Manage 1995;297–314. http://dx.doi.org/10.1016/0196-8904(95)98895-T.

[30] Leonard BP. A stable and accurate convective modelling procedure based on quadratic upstream interpolation. Comput Methods Appl Mech Engrg 1979;19(1):59–98. http://dx.doi.org/10.1016/0045-7825(79)90034-3.

[31] Palsson H. Methods for planning and operating decentralized combined heat and power plants (Ph.D. thesis), Risø & DTU, Department of Energy Engineering (ET); 2000, p. 199.

[32] Giraud L, Baviere R, Vallée M, Paulus C. Presentation, validation and application of the DistrictHeating modelica library. In: Proceedings of the 11th international modelica conference, Versailles, France, September 21-23, 2015. Versailes; 2015, p. 79–88. http://dx.doi.org/10.3384/ecp1511879.

[33] Wetter M, Zuo W, Nouidui TS, Pang X. Modelica buildings library. J Build Perform Simul 2014;7(4):253–70. http://dx.doi.org/10.1080/19401493.2013.765506.

[34] Klein SA, Beckman WA, Mitchell JW. TRNSYS – A transient system simulation program. 1997.

[35] Wang H, Meng H. Improved thermal transient modeling with new 3-order numerical solution for a district heating network with consideration of the pipe wall's thermal inertia. Energy 2018;160:171–83. http://dx.doi.org/10.1016/j.energy.2018.06.214.

[36] Wen CY, Fan LT. Models for flow systems and chemical reactors, Vol. 3rd. New York: Marcel Dekker, Inc; 1975.

[37] Skoglund T, Dejmek P. A dynamic object-oriented model for efficient simulation of fluid dispersion in turbulent flow with varying fluid properties. Chem Eng Sci 2007;62(8):2168–78. http://dx.doi.org/10.1016/j.ces.2006.12.067.

[38] Meibodi SS, Rees S, Yang D. Modelling the dynamic thermal response of turbulent fluid flow through pipelines. In: Proceedings of the international building performance simulation association, Vol. 16. 2019, p. 1357–64. http://dx.doi.org/10.26868/25222708.2019.210473.

[39] Hanby VI, Wright JA, Fletcher DW, Jones DNT. Modeling the dynamic response of conduits. HVAC R Res 2002;8(1):1–12.

[40] Rees SJ. An extended two-dimensional borehole heat exchanger model for simulation of short and medium timescale thermal response. Renew Energy 2015;83:518–26. http://dx.doi.org/10.1016/j.renene.2015.05.004.

[41] He M. Numerical modelling of geothermal borehole heat exchanger systems (Ph.D. thesis), (December). Leicester, UK: De Montfort University; 2011.

[42] Meibodi SS, Rees S. Dynamic thermal response modelling of turbulent fluid flow through pipelines with heat losses. Int J Heat Mass Transfer 2020;151:119440. http://dx.doi.org/10.1016/j.ijheatmasstransfer.2020.119440.

[43] Skoglund T, Årzén KE, Dejmek P. Dynamic object-oriented heat exchanger models for simulation of fluid property transitions. Int J Heat Mass Transfer 2006;49(13–14):2291–303. http://dx.doi.org/10.1016/j.ijheatmasstransfer.2005.12.005.

[44] Abugabbara M, Javed S, Johansson D. A simulation model for the design and analysis of district systems with simultaneous heating and cooling demands. Energy 2022;261(PA):125245. http://dx.doi.org/10.1016/j.energy.2022.125245.

[45] Hirsch H, Nicolai A. An efficient numerical solution method for detailed modelling of large 5th generation district heating and cooling networks. Energy 2022;255:124485. http://dx.doi.org/10.1016/j.energy.2022.124485.

[46] Claesson J. Dynamic thermal networks. Outlines of a general theory. In: Proceedings of the 6th symposium on building physics in the nordic countries Trondheim, Norway. Trondheim, Norway; 2002, p. 47–54.

[47] Rees S, Van Lysebetten G. A response factor approach to modelling long-term thermal behaviour of energy piles. Comput Geotech 2020;120. http://dx.doi.org/10.1016/j.compgeo.2019.103424.

[48] Fan D, Rees SJ, Spitler JD. A dynamic thermal network approach to the modelling of Foundation Heat Exchangers. J Build Perform Simul 2013;6(2):81–97. http://dx.doi.org/10.1080/19401493.2012.696144.

[49] Shafagh I, Rees S, Mardaras IU, Janó MC, Carbayo MP. A model of a diaphragm wall ground heat exchanger. Energies 2020;13(2):1–23. http://dx.doi.org/10.3390/en13020300.

[50] Rees SJ, Fan D. A numerical implementation of the Dynamic Thermal Network method for long time series simulation of conduction in multi-dimensional non-homogeneous solids. Int J Heat Mass Transfer 2013;61(6):475–89. http://dx.doi.org/10.1016/j.ijheatmasstransfer.2013.02.016.

[51] Wentzel E. Thermal modeling of walls, foundations and whole buildings using dynamic thermal networks (Ph.D. thesis), Chalmers University of Technology; 2005, p. 221.

[52] Claesson J. Dynamic thermal networks. background studies i: elements of a mathematical theory of thermal responses. Göteborg, Sweden: Chalmers University of Technology, Departmental Report; 2002.

[53] Claesson J. Dynamic thermal networks: a methodology to account for time-dependent heat conduction. In: Proceedings of the 2nd international conference on research in building physics, Leuven, Belgium. 2003, p. 407–15.

[54] Strand RK. Heat source transfer functions and their application to low temperature radiant heating systems (Ph.D. thesis), University of Illinois at Urbana-Champaign; 1995.

[55] Bergman TL, Lavine AS, Incropera FP. Fundamentals of heat and mass transfer. 7th ed.. John Wiley & Sons, Incorporated; 2011.

[56] Skoglund T, Dejmek P. A dynamic object-oriented model for efficient simulation of microbial reduction in dispersed turbulent flow. J Food Eng 2008;86(3):358–69. http://dx.doi.org/10.1016/j.jfoodeng.2007.10.013.

[57] Weller HG, Jasak H, Tabor G. A tensorial approach to computational continuum mechanics using object-oriented techniques. Comput Phys 1998;12(6):620–31.

[58] Ciuprinskas K, Narbutis B. An experimental investigation of heat losses in the district heating network. Energetika 1999;2:35–40.

[59] Gabrielaitiene I, Bøhm B, Sunden B. Evaluation of approaches for modeling temperature wave propagation in district heating pipelines. Heat Transf Eng 2008;29(1):45–56. http://dx.doi.org/10.1080/01457630701677130.

[60] S. Meibodi S, Rees S. Experimental validation of the dynamic thermal network approach in modeling buried pipes. Sci Technol Built Environ 2023;1–17. http://dx.doi.org/10.1080/23744731.2023.2222622.

[61] Bavière R, Giraud L, Vallée M, Paulus C. Presentation, validation and application of the district heating modelica library. In: Proceedings of the 11th international modelica conference, Versailles, France, September 21-23. 2015, p. 11. http://dx.doi.org/10.3384/ecp1511879.